Study on Flexural Capacity and Deformation of Partially Filled Steel-Fiber Lightweight Concrete Composite Beams

Chenyang Ding[1], Xu Yan[2*] and Wei Sun[3]

[1, 2, 3] School of Civil Engineering, Shenyang Jianzhu University, Shenyang, Liaoning, 110168, China

[1]2692549693@qq.com,[2]cexyan@sjuz.edu.cn,[3]Lg1_315@126.com

Abstract. In order to give full play to the performance of light weight and high strength of steel-concrete composite members, this paper proposes a partially filled steel-fiber volcanic slag aggregate concrete composite beam. Through the bending static test and finite element analysis of three rectangular cross-section beam specimens, the influence of filling fiber and changing the flange width-thickness ratio parameters on the bending mechanical properties and failure modes of composite beams was studied.

Keywords: Steel reinforced concrete composite members ; bending static test ; bending performance.

1 Introduction

Partially Encased Composite Structure (hereinafter referred to as PEC[1]) is mainly formed by pouring concrete between the flanges and both sides of the web by H-shaped steel. However, based on a large number of studies on PEC members [2-6], it is found that the core concrete is mainly ordinary concrete. Due to the characteristics of ordinary concrete, such as self-weight and poor ductility, the light weight and high strength performance of the steel itself is limited, and the fiber can improve the above deficiencies. Therefore, this paper proposes a partially filled steel-fiber volcanic slag aggregate concrete composite (hereinafter referred to as PELWC) structure, and uses bending static test to study the influence of fiber and flange width-thickness ratio on the flexural bearing capacity, ductility and failure mode of PELWC beams during bending.

2 Test Survey

2.1 Test Raw Materials and Mix Ratio

The test concrete is PELWC30 hybrid fiber volcanic slag concrete, and the mix ratio of concrete is shown in Table 1. The Q235 steel is used to roll the steel, and the ultimate

A. S. B. A Rashid et al. (eds.), *Proceedings of the 2024 3rd International Conference on Applied Mechanics and Engineering Structures (AMES 2024)*, Advances in Engineering Research 34,
https://doi.org/10.2991/978-94-6463-473-0_19

tensile strength and elastic modulus corresponding to 6mm and 12mm are 435Mpa, 404Mpa and 210Gpa, 206Gpa, respectively. Two rows of HRB300 transverse tie rods with a diameter of 10 mm are welded in the middle of the upper and lower flanges of the section steel, and the corresponding ultimate tensile strength and elastic modulus are 433 MPa and 205 GPa, respectively.

Table 1. Concrete mix

Concrete type	42.5 Ordinary Portland cement / kg	River sand / kg	Volcanic slag / kg	Water / kg	Polycarboxylate superplasticizer / kg	Polypropylene fiber / kg	Steel fiber / kg	42.5 fast hardening sulphoaluminate cement / kg
LWC30	117	234	167	60	1	4.5	5	16.7
LC30	39	78	55	20	0.33	—	—	5.5

2.2 Test Scheme

Three PELWC beam contrast specimens were designed in the test. The specimen structure of each beam is shown in Figure 1, the loading device is shown in Figure 2 and the parameter design is shown in Table 2. In the test, the four-point symmetrical monotonic static loading method is adopted, and the load is evenly transmitted to the top of the specimen by the distribution beam, as shown in Figure 2. Before loading, the preloading test is carried out in the elastic range. After the preloading is completed, the loading is carried out step by step with 1 / 10 of the simulated test load value as the first level, and each level is loaded for 3 minutes. When the specimen enters the yield state, it is adjusted to the displacement loading control. During the period, the specimen is observed and recorded. When the mid-span displacement of the specimen reaches 1 / 50 of the span, the loading is stopped.

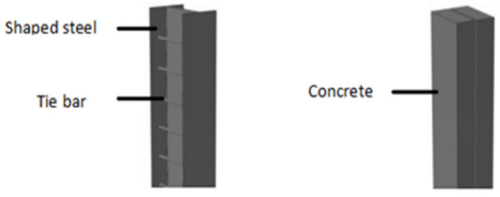

Fig. 1. Basic structure of PELWC beam

Fig. 2. Testing apparatus

Table 2. Design parameters of specimens

Specimen number	$b \times h \times t_w \times t_f$ /mm	L /m	Flange width-thickness ratio	λ	Type and strength of concrete
LC-1-1L	150*200*6*6	2.0	11	3.0	LC30
LWC-1-2L	150*200*6*6	2.0	11	3.0	LWC30
LWC-1-3L	150*200*6*12	2.0	5.25	3.0	LWC30

Note: LC-1-1L is a fiber-free PEC beam, LWC-1-2L and LWC-1-3L are hybrid fiber PEC beams; L is the span of the specimen; b is the width of the cross section; t_w is the width of H-beam web; t_f is the flange width of H-beam; h is the effective height of the section; a is the length of shear span; λ is the shear span ratio, $\lambda = a / h$.

3 Test Results and Analysis

3.1 Failure Phenomenon and Load Deflection Curve

Bending failure occurred in all three PELWC beam specimens, and the stress process of the three specimens was basically the same. The load − mid-span deflection curves of each specimen are shown in Figure 3, and the main test results are shown in Table 3. It can be seen from Figure 3 that all beam specimens can be divided into three stages from the beginning of loading to bending failure.

1) In the elastic working stage, concrete and steel are subjected to force together until the specimen cracks, and the load and mid-span deflection also increase linearly.

2) In the cracking stage of the specimen, the load-deflection curve began to show a nonlinear change until the lower flange of the steel was subjected to tensile yield.

3) In the failure stage of the specimen, with the increase of load, the deflection of the beam also increases rapidly. The deflection of the specimen LWC1-2L is greater than that of LC1-1L, indicating that the addition of fiber contributes to the improvement of ductility. The deflection of the specimen LWC1-3L is greater than that of LWC1-2L, indicating that reducing the width-to-thickness ratio of the flange also contributes to the improvement of ductility. When the test stops, the concrete in the tensile zone breaks, but its bearing capacity does not decrease, indicating that the concrete on the tensile side has little effect on the bearing capacity of the component.

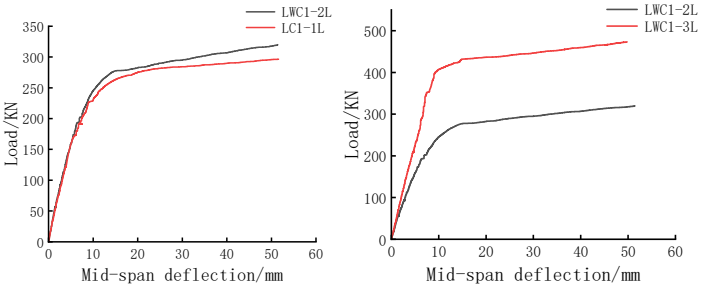

Fig. 3. Load-midspan deflection relation curve

Table 3. Bearing capacity and displacement of characteristic points

Specimen number	P_{cr}/kN	P_y/kN	P_u/kN	δ_y/mm	δ_u/mm	μ
LC-1-1L	80	262	287	14.28	36	2.52
LWC-1-2L	91	278	302	16.32	36	2.21
LWC-1-3L	95	411	454	9.91	36	3.63

Note: P_{cr} is cracking load; P_y is yield load; P_u is the ultimate load; δ_y is the mid-span deflection

when the yield load is reached; δ_u is the mid-span deflection when reaching the ultimate load; μ is the displacement ductility coefficient, $\mu=\delta_u/\delta_y$.

1) Bearing capacity analysis

It can be seen from Table 1 and Table 3 that the ultimate bearing capacity of LWC1-2L is 5.23 % higher than that of LC1-1L, indicating that the addition of 1 % polypropylene fiber and 1.1 % steel fiber only contributes to the improvement of the bearing capacity of PELLWC beam specimens, but the effect is not significant.

It can be seen from Table 1 and Table 3 that with the decrease of the flange width-to-thickness ratio, the ultimate bearing capacity of the specimen LWC1-3L is 50.33 % higher than that of LWC1-2L, indicating that the reduction of the flange width-to-thickness ratio has made an important contribution to the improvement of the bearing capacity of the PELLWC beam specimen, which is similar to the research results of other scholars [7-8].

2） Ductility

The ductility coefficient μ is used to measure the ductility performance of the component: $\mu=\delta u/\delta y$.

In the formula : δu is the limit displacement, δy is the yield displacement.

It can be seen from Table 3 that the ductility coefficient of the specimen LWC-1-2L is 14.03 % higher than that of LC-1-1L, indicating that the addition of fiber can improve the ductility of the component. In addition, the ductility coefficient of the specimen LWC-1-3L is 64.25 % higher than that of LWC-1-2L, indicating that the smaller the flange width-to-thickness ratio of the specimen, the better the ductility.

4 Numerical Simulation Analysis of PELWC Beam

4.1 The Establishment of Material Constitutive and Finite Element Model

In this paper, the steel is Q235, the steel of the simulated specimen is calculated according to the basic properties of the test specimen, and the steel model uses the elastic-plastic model [9]. The compressive stress-strain curve of concrete is based on the compressive constitutive model of steel fiber volcanic slag concrete proposed by Tao Yu of Jilin Jianzhu University [10]. The uniaxial tensile stress-strain curve of concrete is based on the tensile constitutive model of steel polypropylene hybrid fiber concrete adopted by Mei Guodong of Wuhan University [11] and others in the study. The PELWC beam model of the specimen adopts the 8-node hexahedral element C3D8R, and the boundary conditions are applied according to the fabrication mode of the simply supported beam.

4.2 Finite Element Parameter Expansion Analysis

In order to prove the influence of the flange width-to-thickness ratio on the ultimate bearing capacity of the beam specimen, the following two groups of specimens were designed in the finite element simulation for verification, as shown in Table 4.The load-span deflection curve of the PELWC beam is shown in Figure 4.

Table 4. The design parameters of the specimen and the bearing capacity of the feature points

Specimen number	$b \times h \times t_w \times t_f$/mm	L /m	Flange width-thickness ratio	λ	Pu/ kN	range of load capacity improvement%
LWC-2-1L	150*200*6*8	2.0	8.3	3	320	—
LWC-2-2L	150*200*6*10	2.0	6.5	3	392	22.5
LWC-2-3L	150*200*6*16	2.0	3.8	3	455	16.07
LWC-3-1L	200*200*6*6	2.0	15.17	3	359	—
LWC-3-2L	200*200*6*10	2.0	9	3	467	30.8
LWC-3-3L	200*200*6*20	2.0	4.15	3	488	4.5

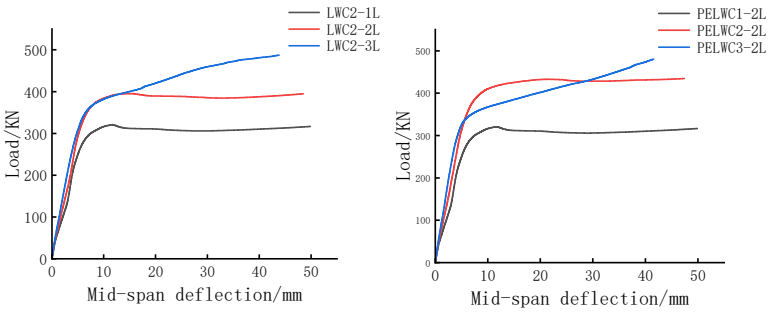

Fig. 4. Load-midspan deflection relation curve

It can be seen from Figure 4 that the bending ultimate bearing capacity of the two groups of specimens LWC-2-1L, LWC-2-2L, LWC-2-3L and LWC-3-1L, LWC-3-2L, LWC-3-3L increases in turn when they reach the test failure standard. The results show that with the decrease of the width-to-thickness ratio of the flange, the bending ultimate bearing capacity gradually increases, but it can be seen from the data in Table 4 that the increase is getting smaller and smaller. This is because the farther the flange is from the web, the smaller the degree of force it participates in, and the wider the flange is, the only part near the web can effectively bear the load.

5 Conclusion

1) When the deflection of the PELWC beam reaches the failure standard, the concrete in the tension zone breaks, but its bearing capacity does not decrease, indicating that the concrete on the tension side has little effect on the bearing capacity of the member.

2) The width-to-thickness ratio of section steel flange has a significant effect on the ultimate bearing capacity and ductility of PELWC beams. Fiber has a certain effect on the ultimate bearing capacity, but the effect is not obvious. It is suggested that the flexural capacity of PELWC beams can be improved by increasing the width-to-thickness ratio of section steel flange in engineering application.

3) With the decrease of the width-to-thickness ratio of the flange, the flexural ultimate bearing capacity of the PELWC beam gradually increases, but the increase is getting smaller and smaller, indicating that a part of the thickness near the web can effectively bear the load.

References

1. T / CECS 719-2020 Technical specification for partially encased steel-concrete composite structures [S].
2. HY Li, SP Chen, YF Lu.Study on flexural behavior of partially reinforced steel fiber reinforced concrete beams with BFRP bars [J].Concrete, 2022, (09) : 62-65 + 71.
3. CHI Y, XU L, ZHANG Y. Experimental study on hybrid fiber-reinforced concrete subjected to uniaxial compression[J]. Journal of Materials in Civil Engineering, 2014, 26（2）：211-218.
4. ASSI I M，ABED S M，HUNAITI Y M. Flexural strength of composite beams partially encased in lightweightconcrete[J]. Pakistan Journal of Applied Sciences, 2002, 2(3) : 320-323.
5. L. G. Sorelli, A. Meda, G. A. Plizzari. Bending and Uniaxial Tensile Tests on Concrete Reinforced with Hybrid Steel Fibers[J]. Journal of Materials in Civil Engineering, 2005, 17 (05). 519-527.
6. Farhad Aslani, Shami Nejadi. Self-compacting concrete incorporatin steel and polypropylene fibers: Compressive and tensile strengths, moduli of elasticity and rupture, compressive stress-strain curve, and energy dissipated under compression[J]. Composites Part B.
7. NAAMAN A E. Rectangular stress block and T-section behavior [C] / / Open Forum：Problems and Solutions，PCI Journal，2002，47 (5)：106-112.
8. SEGUIRANT S J, BRICE R, KHALEGHI B. Flexural strength of reinforced and prestressed concrete T-beams [J]. PIC Journal,2005, 50 (1) : 44-73.
9. Code for design of concrete structures : GB 50010-2010 [S]. 2015 edition. Beijing : China Construction Industry Press, 2015
10. Y Tao. Study on mechanical properties and axial compression constitutive relationship of steel fiber volcanic slag concrete after high temperature [D]. Jilin Jianzhu University, 2022.
11. GD Mei. Study on uniaxial tensile properties and constitutive relationship of steel-polypropylene hybrid fiber reinforced concrete [D].Wuhan University, 2014.